Proceedings of the 17th World Congress
The International Federation of Automatic Control
Seoul, Korea, July 6-11, 2008

Deployment of Mobile Sensor Networks with Discontinuous Dynamics

Jaeyong Lee * **Suhada Jayasuriya** **

* *Mechatronics Center, Institute of Industrial Technology, Samsung Heavy Industries, Daejeon 305-380, KOREA (e-mail: jyec.lee@samsung.com).*
** *Department of Mechanical Engineering, Texas A&M University, TX 77840, USA (e-mail: sjayasuriya@tamu.edu)*

Abstract: In this paper, we analyze the stability of a network that uses piecewise smooth potential functions. A gravitation-like force is applied to deploy a group of agents and to form a certain configuration. We use a nonsmooth version of the Lyapunov stability theory and LaSalles invariance principle to show asymptotic stability of the network which is governed by discontinuous dynamics. Hexagonal deployment using such a force is shown through simulation.

1. INTRODUCTION

The sensor location problem in mobile sensor networks has similarities to the conventional art gallery problem (AGP) studied in computational geometry [1]. AGP seeks to determine how to use a minimal number of guards (cameras) in a polygon so that every point in the polygon is observed by at least one guard (camera). However, the solutions of AGP cannot be directly applied to the mobile sensor network deployment problem. First, AGP solutions assumes that the model of a environment can be well constructed *a priori*. This is not typical in mobile sensor network deployment. Secondly, AGP solutions suppose that a guard can observe as long as a line-of-sight exists, while sensors usually have finite sensing ranges. Furthermore, AGP solutions do not consider the limitations imposed by communication range.

The problems of coverage and deployment are fundamentally interrelated. In [2], the authors have discussed the problem of location and deployment of sensors from a coverage standpoint. The authors define the coverage problem from different points of view, including deterministic, statistical, and the worst and best cases. The goal is to have each location in the environment covered by at least one sensor. They argue that coverage is a primary performance metric that determines quality-of-service (QoS) and combined computational geometry and graph theory for their algorithms.

The concept of coverage as a paradigm for the system-level functionality of multirobot systems was introduced by Gage [3]. Gage defines three basic types of coverage: (i) Blanket, (ii) Barrier, and (iii) Sweep coverage. In *Blanket coverage*, the objective is to accomplish a static arrangement of nodes that maximizes the total detection area. The objective of *Barrier coverage* is to minimize the probability of undetected penetration through the barrier. *Sweep coverage* is roughly equivalent to the moving *Barrier coverage*. According to this taxonomy, the deployment problem in this research is equivalent to blanket coverage.

Autonomous mobile sensor deployment algorithms have been intensively researched. One of the most widely used methods is to employ artificial force concept between mobile agents. Since first presented by Khatib [4], potential field based methods have been extensively used in path planning. In potential field based algorithms [5] [6] [7], a control law is defined as the negative gradient of the potential. Popa *et al*. [8] deployed sensor networks using conventional potential field method. Voronoi diagram method has also been used to generate artificial forces [9]. On applying these algorithms, the mobile sensor nodes get situated in the environment in a distributed manner. A Virtual force can be directly derived to enhance network coverage for randomly placed sensors as developed by [10].

Most of the previous researches, however, assumed a smooth potential field which is differentiable over the entire region. This assumes two properties. First assumption is that a neighboring set (a set of nodes with which a node can communicate) of a node never changes, and the second is that a potential function is differentiable. A force field derived from a smooth potential function becomes continuous, and the system is governed by continuous dynamics.

We remove the second assumption on the continuity of a force field. We develop a system represented by differential equations with discontinuous right hand side, where interactive forces between nodes are discontinuous. We followed the framework by Shevitz and Paden [11] to prove stability. The main advantage of this work is to grant much freedom in designing a force field or shaping a potential field for a network formation.

2. SENSOR NETWORK DEPLOYMENT

2.1 Optimal Sensor Locations

An important phase in the operation of a sensor network is the deployment of sensors in a field of interest. It is a critical issue because it directly affects the cost and detection capability of a wireless sensor network. Sensor

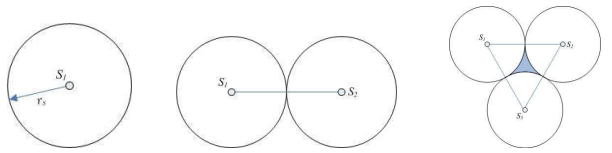

(a) disk type sensor model (b) 2 sensors (c) 3 sensors with coverage hole

Fig. 1. Sensor model and coverage

deployment has received considerable attention recently. Critical goals during deployment of a sensor network include coverage, connectivity, and load balancing among others.

The deployment strategy for sensor networks varies with the application considered. It can be predetermined when the environment is sufficiently known and under control, in which case the sensors can be strategically deployed manually.

The deployment can also be *a priori* undetermined when the environment is unknown or hostile, such as remote harsh fields, disaster areas and toxic urban regions. In this case, sensor deployment cannot be pre-planned and performed manually. For example, the sensors may be airdropped from an aircraft or deployed by other means, generally resulting in a random placement. Random placement of sensors in a target area is often desirable especially if no *a priori* knowledge of the terrain is available. Random deployment is practical in military applications, where sensor networks are initially established by dropping or throwing sensors into a desired field. However, such random deployment does not always lead to effective coverage, especially if the sensors are overly clustered and there is a small concentration of sensors in certain parts of the sensor field. The actual landing position cannot be controlled due to the existence of wind and obstacles such as trees and buildings. Consequently, the coverage may be inadequate for specific application requirements regardless of how many sensors are dropped.

In these scenarios, it is possible to make use of mobile sensors, which can can be made to move to appropriate locations to provide the required coverage. Mobility can significantly increase the capability of a sensor network by making it resilient to failures, react to events, and be able to support disparate missions with a common set of sensors. Multiple mobile agents provide us with a flexible, robust and distributed solution for data collection in sensor networks.

Sensor deployment is basically an optimal sensor location problem. Let us consider a binary sensor model which is a disk model as shown in fig. 1(a), and define r_s as its sensing range. The aim of the sensor network is to maximize the area covered by placing multiple sensors in the environment. When there are more than 2 sensors, an optimization problem arises. For example, we can maximize the coverage area by arranging two disks adjacent to each other as shown in fig. 1(b). With more than 3 sensors, which is generally true in sensor networks, there may exist a coverage hole (void) between sensors as shown in fig. 1(c) (colored area in the middle of the three sensors). To remove this void, we may overlap sensor detection areas. In this case, we need to minimize the overlapped area to maximize the covered area for a given number of sensors.

Let us define d_s as the distance between two sensors. Then,

$$d_s = \sqrt{(x_i - x_j)^2 + (y_i - y_j)^2}, \tag{1}$$

where (x_i, y_i) and (x_j, y_j) are two sensor positions in 2-D space. In a two sensor case, it is simply $2r_s$ to maximize coverage area and minimize the communication range. Let us now consider the triangle shown in fig. 2(a). As every d_s is the same, the triangle is an equilateral and from simple geometry, we know d_s is $\sqrt{3}r_s$. The optimal placement of sensors is then the traditional circle packing problem for circles whose radii are $\frac{\sqrt{3}r}{2}$ [12, 13]. A circle packing

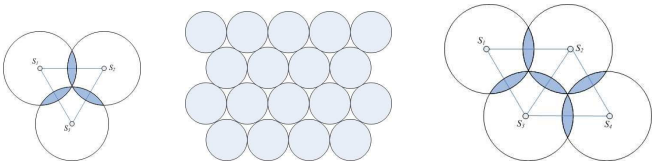

(a) 3 sensors without hole (b) circle packing (c) 4 sensors

Fig. 2. Coverage problem to disk packing

is an arrangement of circles inside a given boundary such that no two overlap and some (or all) of them are mutually tangent. The densest packing of circles in the plane is the regular hexagonal lattice arrangement, which has a packing density of $\frac{\sqrt{3}\pi}{6}$ as shown in fig. 2(b). The overlapped area (A_o) between two circle in fig. 2(a) is $2(\frac{\pi}{6} - \frac{\sqrt{3}}{4})r^2$. In case of four sensors, there are 5 overlapped area as in fig. 2(c).The optimal deployment minimizes such an overlapped area.

2.2 Hexagonal deployment

We have so far shown that a hexagonal structure is optimal in terms of our coverage definition. The main problem now is how one should propagate the hexagonal configuration in a distributed manner.

To successfully reach the goal of networked systems, mobile nodes should communicate with each other. In general, a mobile sensor node has a limited range of communication. Therefore, only nodes which are sufficiently close to each other, can establish communication, and the communication topology is strongly influenced by node motion.

Let x_i be the position vector of the i-th node in 2-D and N be the number of nodes, and assume each node has standard second order linear dynamics. We can define $r_{ij} = |x_{ij}|$ as the distance between the i-th node and the j-th node, and we construct a potential function $\mathrm{V}(r_{ij})$, which is a function of the distance between two nodes. The control input to a node is the force F_{ij} exerted on the i-th node by the j-th node. It is useful to write the force as the negative gradient of the potential field. Therefore, the total force on each node can be described as

$$F_i = \sum_{j \neq i}^{N} F_{ij} = -\sum_{j \neq i}^{N} \nabla \mathrm{V}(r_{ij}). \tag{2}$$

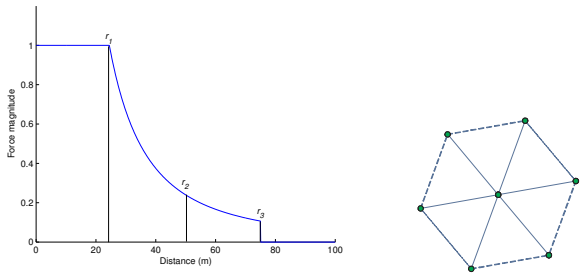

(a) (b)

Fig. 3. Force model and hexagonal structure

The magnitude of the force as a function of the distance is shown in fig. 3. It is necessary to adjust the magnitude of the force to the feasible level to accommodate control input saturation. This limit is set as F_{max}, and comes into play when $r \leq r_1$. The force is repulsive if $r \leq r_2$, and attractive if $r \geq r_2$. There is no force exerted if $r \geq r_3$. In this work, the potential field is chosen so that the force function is of the form

$$F_{ij} = \frac{\alpha}{r_{ij}^{\beta}}, \tag{3}$$

where α and β are the parameters we can tune. Each node uses exactly the same control law because the nodes are assumed to be identical, and are influenced only by the neighboring nodes, i.e., those within a ball of radius r_3. The global minimum of the sum of all the potentials consists of a configuration in which neighboring nodes are spaced equally at a distance r_2 from one another as shown in fig. 3(b).

For a uniform distribution of the sensor nodes, the hexagonality of a deployment can be measured by uniformity. Uniformity is defined as the average of the local standard deviation of the distances between neighboring nodes [14]. Let $\mathcal{N}_i$ be a set of nodes which can communicate with and be detected by the i-th node. Then, the overall uniformity of a deployment is

$$U = \frac{1}{N}\sum_{i=1}^{N} U_i$$
$$U_i = \left(\frac{1}{|\mathcal{N}_i|}\sum_{j\in\mathcal{N}_i}(|x_{ij}| - \mu_i)^2\right)^{\frac{1}{2}}$$

where U_i is the local uniformity, and μ is the mean of the distances between the i-the node and its neighbors. A smaller value of U means that the nodes are more uniformly placed, and with our force model, the deployment has a hexagonal structure.

The main problem of this form of artificial force is that the system has discontinuous right hand side. The sign of the force switches at a certain distance r_2. A node is locally interacting with neighbors, and each node is governed by discontinuous differential equations. Therefore, stability analysis is required for the overall network.

3. STABILITY ANALYSIS FOR TIME INVARIANT SYSTEM

We define the state of the n nodes as

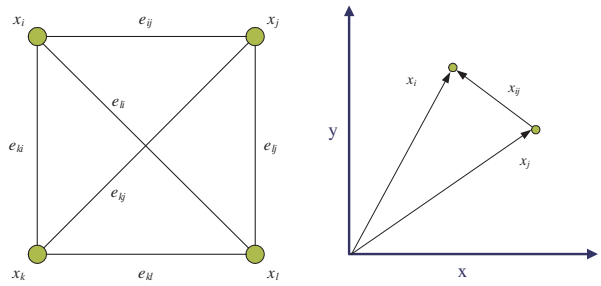

(a) Undirected graph (b) Spacial representation

Fig. 4. Undirected graph and its spacial representation

$$x = (x_1, ..., x_n, \dot{x}_1, ..., \dot{x}_n).$$

Let us consider an undirected neighboring graph, $\mathcal{G} = \{\mathcal{V}, \mathcal{E}\}$, which is composed of as a finite non-empty set of vertices, $\mathcal{V} = \{x_1, x_2, ..., x_n\}$, and a finite set of edges, $\mathcal{E} = \{e_{ij} | (x_i, x_j) \in \mathcal{V} \times \mathcal{V}, x_i \sim x_j\}$ (fig. 4). A vertex represents a mobile node and an edge contains unordered pairs of nodes that depict neighborhood between the nodes. We now define a neighboring set of node i, $\mathcal{N}_i = \{j | (x_i, x_j) \in \mathcal{E}, |x_i - x_j| \leq r_r, r_c\}$, as a set of nodes which can communicate with and be detected by node i. It is proved that if $r_c \geq 2r_r$, complete coverage of a convex region implies connectivity of an arbitrary network [15]. We assume the same condition here so that connectivity is always guaranteed.

First, we consider the time invariant case, where a node can communicate with all other nodes or a set of neighboring nodes $\mathcal{N}_i$ does not change. This property induces that the total potential energy of the group is differentiable as long as the potential energy function for each node is differentiable. Then the control input to a node is smooth and classic Lyapunov stability theory can be applied.
Let us consider a continuously differentiable Lyapunov function (Φ) that combines kinetic energy and potential energy in the form

$$\Phi = \frac{1}{2}\sum_{i=1}^{n}\left(\dot{x}_i^T \cdot \dot{x}_i + \sum_{j\in\mathcal{N}} V(x_{ij})\right). \tag{4}$$

Let us define a set Ω as

$$\Omega = \{(x, \dot{x}) | \Phi \leq \phi\}, \forall\, i, j \in \{1, ..., n\}, \tag{5}$$

for a sufficiently large value of ϕ. The set, for $\phi > 0$, is closed by continuity. Because of the symmetric property of $V(x_{ij})$ and $V(x_{ji})$, and the property of $x_{ij} = -x_{ji}$,

$$\frac{\partial V_{ij}}{\partial x_{ij}} = \frac{\partial V_{ij}}{\partial x_i} = -\frac{\partial V_{ij}}{\partial x_j} \tag{6}$$

Therefore, the time derivative of the potential energy becomes

$$\frac{d}{dt}\sum_{j\in\mathcal{N}} V(x_{ij}) = \sum_{j\in\mathcal{N}}(\dot{V}_{ij}) = \sum_{j\in\mathcal{N}} \dot{x}_{ij}^T \nabla V(x_{ij}) \tag{7}$$
$$= 2\sum_{j\in\mathcal{N}} \dot{x}_i^T \cdot \nabla V(x_{ij}). \tag{8}$$

And, the time derivative of Φ becomes

$$\dot{\Phi} = \sum_{i=1}^{n} \dot{x}_i^T \cdot \left(\ddot{x}_i + \sum_{j \in \mathcal{N}} \nabla V(x_{ij}) \right). \quad (9)$$

For simplicity, let us consider a simple unit mass dynamics system for a node.

$$\ddot{x}_i = u_i - c\dot{x}_i. \quad (10)$$

Because we are considering control input u as the negative gradient of the potential, equation 9 can be expressed as

$$\dot{\Phi} = \sum_{i=1}^{n} \dot{x}_i^T \cdot \left(-c\dot{x}_i - \sum_{j \in \mathcal{N}} \nabla V(x_{ij}) + \sum_{j \in \mathcal{N}} \nabla V(x_{ij}) \right)$$
$$= -c \sum_{i=1}^{n} \dot{x}_i^T \cdot \dot{x}_i.$$

For the positive damping coefficient c, $\dot{\Phi}$ is semi-negative definite ($\dot{\Phi} \leq 0$). Equality $\dot{\Phi} = 0$ holds only when $\dot{x}_i = 0$. Therefore, the system with the given control law is asymptotically stable. Let $\mathcal{S}$ be the invariant set in Ω

$$\mathcal{S} = \{(x, \dot{x}) | \dot{\Phi} = 0\}. \quad (11)$$

From LaSalle's invariance principle, we can conclude that the nodes will converge to the largest invariant set in $\mathcal{S}$. However, with nonzero c, $\dot{\Phi}$ is zero only when all the nodes are at rest. We do not consider the trivial case, in which a node is at rest because there is no node within given sensing range. Therefore, the above statement means that all the distances of neighboring nodes are the same, where the local minima of the potentials are achieved.

4. DISCONTINUOUS DYNAMIC SYSTEMS

Let us again consider each node with unit mass, and define the state variable

$$\mathbf{x} = [x_1, \dot{x}_1, ..., x_i, \dot{x}_i, ..., x_n, \dot{x}_n]^T$$

where $\mathbf{x}_i = [x_i, \dot{x}_i]^T$. Then the agent dynamics can be given by

$$\dot{\mathbf{x}}_i = \psi(\mathbf{x}) + \tau(\mathbf{x}) = f(\mathbf{x}),$$

where $\psi(\mathbf{x})$ is a friction force proportional to the velocity, and $\tau(\mathbf{x})$ is a control input derived from the negative gradient of the system. For the simplest expression,

$$\ddot{x}_i = -c\dot{x}_i - \nabla V,$$

where V is the total potential at x_i due to all the neighboring nodes. The equation appears linear and same as the equation used in the constant topology case which was described in the previous section. However, what we are considering in this section is a system with discontinuous right hand side. In group motion analysis, there are two possibilities that the system has discontinuous dynamics. The first case appears where each node has discontinuous dynamics, while the second case presents the switching topologies where the neighboring set of a node $\mathcal{N}_i$ varies as time passes. We consider the first case here, while methodology and results of nonsmooth analysis are same for the second one. Then the agent dynamics can be explained with a differential inclusion [16]

$$\dot{\mathbf{x}}_i \in K[f](\mathbf{x})_i$$

At the points of discontinuity, $\mathbf{x}$ lies in the convex closure of the liming values of the vector field. Therefore,

$$K[f](\mathbf{x}) = [\dot{x}_i, -c\dot{x}_i - \Sigma_{j \in \mathcal{N}_i} \nabla V_{ij}]$$

Note that we discard sets of measure zero where the gradient of V is not defined. Figure 5 shows the changes

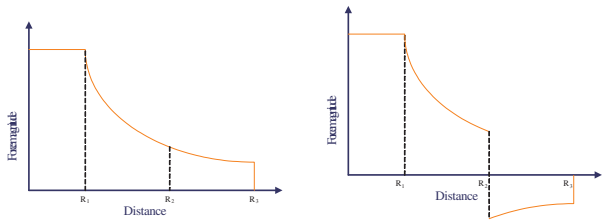

(a) Force model based on gravitational force

(b) Force model between the nodes

Fig. 5. Force model

of the force magnitude corresponding to the distance to a neighbor. It is necessary to refine the magnitude of force to feasible level because of control input saturation. This limit is set as F_{max}, and comes into effect when $r \leq R_1$. The force is repulsive if $r \leq R_2$, and attractive if $r \geq R_2$. There is no force exerted if $r \geq R_3$.

$$F = \begin{cases} F_{max} & \text{if } r < R_1 \\ \dfrac{G}{r^p} & \text{if } R_1 < r < R_2 \\ -\dfrac{G}{r^p} & \text{if } R_2 < r < R_3 \\ 0 & \text{if } R_3 < r. \end{cases}$$

Let us consider the nonnegative Lyapunov function candidate

$$\Phi = \frac{1}{2} \sum_{i=1}^{n} \left(\dot{x}_i^T \cdot \dot{x}_i + \sum_{j \in \mathcal{N}} V(x_{ij}) \right)$$

We now define $V = -\int_r \mathrm{F} dr$, which is a negative form for the conventional potential energy along the path so that control input to the system is a negative gradient of the the potential energy. For the force shown in figure 5, we have following potential energy $(V) =$

$$\begin{cases} -rF_{max} & \text{if } r < R_1, \\ -R_1 F_{max} - \dfrac{G}{\rho} r^\rho + \dfrac{G}{\rho} R_1^\rho & \text{if } R_1 < r < R_2, \\ -R_1 F_{max} - \dfrac{2G}{\rho} R_2^\rho + \dfrac{G}{\rho} R_1^\rho + \dfrac{G}{\rho} r^\rho & \text{if } R_2 < r < R_3, \\ -R_1 F_{max} - \dfrac{2G}{\rho} R_2^\rho + \dfrac{G}{\rho} R_1^\rho + \dfrac{G}{\rho} R_3^\rho & \text{if } R_3 < r, \end{cases}$$

where ρ is $(1 - p)$. First two terms in each region are negative for repulsive force whereas the last integral is positive for attractive force. The graphical representation of the potential is shown in figure 6.

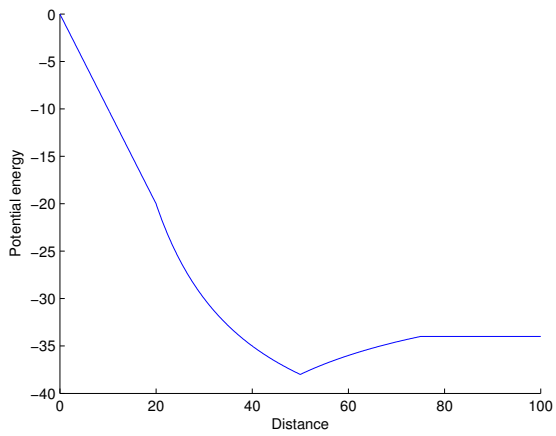

(a) Potential energy in 2D plot

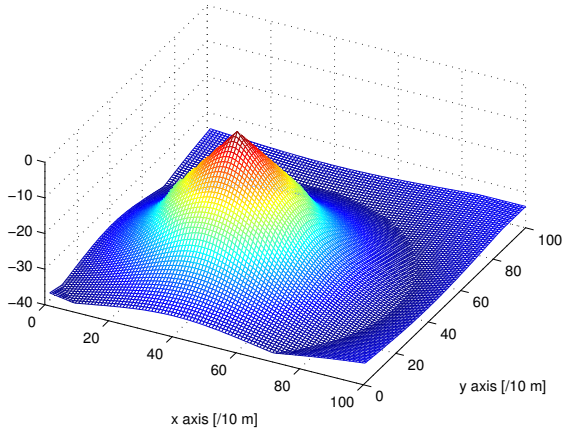

(b) Potential energy in 3D plot

Fig. 6. Potential energy derived from the force law

There are three nonsmooth points in the potential at R_1, R_2, and R_3. The potential values at the discontinuities are

$$\begin{aligned}
V_{R_1} &= -R_1 F_{max} \\
V_{R_2} &= R_1 F_{max} + \frac{G}{(1-p)} R_2^{(1-p)} - \frac{G}{(1-p)} R_1^{(1-p)} \\
V_{R_3} &= -R_1 F_{max} - \frac{2G}{(1-p)} R_2^{(1-p)} \\
&\quad + \frac{G}{(1-p)} R_1^{(1-p)} + \frac{G}{(1-p)} R_3^{(1-p)}
\end{aligned}$$

If the distance between two nodes are one of those nonsmooth points ($r \notin \Omega_v$), we need to consider the generalized time derivative of Φ. To apply the nonsmooth version of Lyapunov stability analysis, we need to check the regularity of Φ.
Let us first establish regularities of V at distances which belong to the set of measure zero.

One sided directional derivatives [17] are defined as

$$f'(R_1, v) = \lim_{t \downarrow 0} \frac{V(R_1 + tv)}{V_{R_1}} = \begin{cases} a < 0 & \text{if } v > 0, \\ b > 0 & \text{if } v < 0. \end{cases}$$

$$f'(R_2, v) = \lim_{t \downarrow 0} \frac{V(R_2 + tv)}{V_{R_2}} = \begin{cases} c > 0 & \text{if } v > 0, \\ d < 0 & \text{if } v < 0. \end{cases}$$

$$f'(R_3, v) = \lim_{t \downarrow 0} \frac{V(R_3 + tv)}{V_{R_3}} = \begin{cases} e = 0 & \text{if } v > 0, \\ f < 0 & \text{if } v < 0. \end{cases}$$

Now we define gradient of V where $r \notin \Omega_v$

$$\nabla V(r) = \begin{cases} -\dfrac{G}{R_1^p} & \text{if } r < R_1 \\ -\dfrac{G}{r^p} & \text{if } R_1 < r < R_2 \\ \dfrac{G}{r^p} & \text{if } R_2 < r < R_3 \\ 0 & \text{if } R_3 < r. \end{cases}$$

Note that ∇V includes the derivative with respect to time even though it is not shown in the expression. By combining definition of Glarke's generalized gradient, we have

$$f^\circ(R_1, v) = \begin{cases} a < 0 & \text{if } v > 0, \\ b > 0 & \text{if } v < 0. \end{cases}$$

$$f^\circ(R_2, v) = \begin{cases} c > 0 & \text{if } v > 0, \\ d < 0 & \text{if } v < 0. \end{cases}$$

$$f^\circ(R_3, v) = \begin{cases} e = 0 & \text{if } v > 0, \\ f < 0 & \text{if } v < 0. \end{cases}$$

By the definition of regular function, V is regular, and Φ is regular as a sum of regular functions. Regularity and the property of finite sums of generalized gradients provide us

$$\partial\Phi = [\Sigma \partial_{x_1} V_i, \dot{x}_i ..., \Sigma \partial_{x_n} V_i, \dot{x}_n]^T$$

From Clarke's chain rule, we have the generalized time derivative of Φ

$$\begin{aligned}
\dot{\tilde{\Phi}} &= \bigcap_{\xi \in \partial\Phi(x(t))} \xi^T \left(K[f](x(t))\right) \\
&= \bigcap \Sigma \left[\dot{x}_i^T \Sigma \partial_{x_i} V - c \dot{x}_i^T \dot{x}_i - \dot{x}_i^T \Sigma \partial_{x_i} V \right] \\
&= \overline{co}\{-\Sigma c \dot{x}_i^T \dot{x}_i\} \\
&\leq 0.
\end{aligned}$$

As we do not consider the trivial case where the graph is not connected, $\dot{\tilde{\Phi}} = 0$ only when $\dot{x}_i = 0$.Let $\mathcal{S}$ be the invariant set in Ω

$$\mathcal{S} = \{(x, \dot{x}) | \dot{\Phi} = 0\}. \tag{12}$$

From LaSalle's invariance principle, we can conclude that the nodes will converge to the largest invariant set in $\mathcal{S}$. However, with nonzero c, $\dot{\Phi}$ is zero only when all the nodes are at rest. We do not consider the trivial case, in which a node is at rest because there is no node within given sensing range. Therefore, the above statement means that all the distances of neighboring nodes are the same, where the local minima of the potentials are achieved.

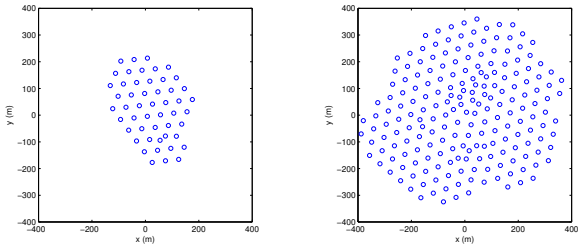

(a) number of nodes: 50 (b) number of nodes: 200

Fig. 7. Hexagonal structure construction

5. SIMULATION RESULTS

Simulation is conducted for the hexagonal formation via the artificial force from potential, and for the hierarchical formation control. The main purpose of this kind of coverage is to get maximum coverage without coverage hole.

Figure 7 shows the results from a hexagonal formation of 50 mobile sensor nodes (fig. 7(a)) and 200 nodes (fig. 7(b)). In this simulation, α and β are 500 and 2, respectively, desired equilibrium distance r_2 is $50m$, and F_{max} is limited to be 1. The sampling time (δt) is 0.1 sec. and the number of iterations is 6000 so that the total time for the deployment is 10 minutes. Figure 7(a) shows an example of a hexagonal formation. Note however, that the hexagonal structure is not perfect. There are a small number of nodes lumped in the lower right corner. The perimeter of the structure is not hexagonal. These defects are inevitable in our potential based force model, because we are not considering a global controller which can shape the whole system. The overall formation shows, however, well-defined hexagons.

6. CONCLUSIONS

A force law inspired by gravitational force was employed to form such a hexagonal structure. Due to the nature of the proposed force law, the stability of the system was analyzed with discontinuous dynamics. A Lyapunov function which combines kinetic energy and potential energy was constructed and a nonsmooth version of Lyapunov stability theory and LaSalle's invariance principle were used to prove stability.

The main contribution of this proof is to expand the mutual relation between the force which is required to have a certain formation and the potential function which is used for the stability analysis. This is because the force is derived by taking the derivative of the potential. In other words, different formations can be achieved with different force laws. The line integral which becomes the potential function is then taken to analyze the stability of the system. This procedure is the inverse of the conventional potential field methods, which first build potential functions and then use the derivative of the potential as a control input. Based on the proof given in this research, a stable system with a desired formation can be achieved.

REFERENCES

[1] O'Rourke, J., *Art Gallery Theorems and Algorithms*, Oxford University Press, New York, August 1987.

[2] S. Meguerdichian, F. Koushanfar, M. Potkonjak, M. Srivastava, "Coverage problems in wireless ad hoc sensor networks," in *Proc. IEEE INFOCOM Conf.*, 2001, pp. 13801387

[3] D. W. Gage, "Command control for many-robot systems," in *the Nineteenth Annual AUVS Technical Symposium*, pages 2224, Hunstville Alabama, USA, June 1992. Reprinted in *Unmanned Systems Magazine*, Fall 1992, Volume 10, Number 4, pp 28-34.

[4] O. Khatib, "Real-time obstacle avoidance for manipulators and mobile robots," *International Journal of Robotics Research,* vol. 5, no. 1, pp. 90-98, 1986.

[5] P. Ogren, E. Fiorelli, N. E. Leonard, "Cooperative control of mobile sensor networks:Adaptive gradient climbing in a distributed environment." *IEEE Transactions on Automatic Control*, vol. 49, no. 8, pp. 1292-1302, Aug. 2004.

[6] R. Bachmyer, N. E . Leonard. "Vehicle Networks for a Gradient Descent in a Sampled Environment," in *Proc. of Conf. on Decicion and Control,* 2002.

[7] S. Paduri and G. Sukhatme, "Constrained Coverage for Mobile Sensor Network," in *Proc. of International Conference on Robotics and Automation,* 2002.

[8] D. O. Popa, C. Helm, H. E.Stephanou, A. Sanderson, "Robotic Deployment of Sensor Networks using Potential Fields," in *Proc. Of International Conference on Robotics and Automation,* 2004.

[9] J. Cortés, S. Martinez, T. Karatas, F. Bullo, "Coverage control for mobile sensing networks," *IEEE Transactions on Robotics and Automation*, vol. 20 no. 2, pp. 243-255, 2004.

[10] Y. Zou and K. Chakrabarty, "Sensor deployment and target localization based on virtual forces," in *Proceedings of IEEE Conference on Computer Communications (INFOCOM)*, 2003.

[11] D. Shevitz, B. Paden, "Lyapunov stability theory of nonsmooth systems," *IEEE Trans. on Automatic Control,* vol. 49, no. 9, pp. 1910-1914, 1994.

[12] M. Locatelli, U. Raber, "Packing equal circles in a square: a deterministic global optimization approach," *Discrete Applied Mathematics*, vol. 122, pp. 139-166, 2002.

[13] P. G. Szabó, T. Csendes, L. G. Casado, I. García, "Packing Equal Circles in a Square I. Problem Setting and Bounds for Optimal Solutions," *New Trends in Equilibrium Systems*, pp. 1-15, 2000.

[14] N. Heo, P. K. Varshney, "Energy-Efficient Deployment of Intelligent Mobile Sensor Networks," *IEEE Transactions on Systems, Man, and CyberneticsPart A: Systems. And Humans*, vol. 35, no. 1, pp. 78-92, 2005.

[15] H. Zhang, J. C. Hou, "Maintaining Sensing Coverage and Connectivity in Large Sensor Networks," in *Ad Hoc & Sensor Wireless Networks,* vol. 1, pp. 89-124, 2005.

[16] A. Filippov. *Differential equations with discontinuous right-hand sides,* Kluwer Academic Publishers, 1988.

[17] F. Clarke, *Optimization and Nonsmooth Analysis,* Addison - Wesley, 1983.